Statistical mechanics of a discrete Schrödinger equation with saturable nonlinearity

Mogens R. Samuelsen, Avinash Khare, Avadh Saxena, and Kim Ø. Rasmussen

Phys. Rev. E **87**, 044901 — Published 17 April 2013

DOI: 10.1103/PhysRevE.87.044901

Statistical Mechanics of a Discrete Schrödinger Equation with Saturable Nonlinearity

Mogens R. Samuelsen,[1] Avinash Khare,[2] Avadh Saxena,[3] and Kim Ø. Rasmussen[3]

[1] *Department of Physics, The Technical University of Denmark, DK-2800 Kgs. Lyngby, Denmark*
[2] *Indian Institute of Science Education and Research (IISER), Pune 411021, India*
[3] *Theoretical Division, Los Alamos National Laboratory, Los Alamos, New Mexico, 87545, USA*

We study the statistical mechanics of the one-dimensional discrete nonlinear Schrödinger (DNLS) equation with saturable nonlinearity. Our study represents an extension of earlier work [Phys. Rev. Lett. **84**, 3740 (2000)] regarding the statistical mechanics of the one-dimensional DNLS equation with a cubic nonlinearity. As in this earlier study we identify the spontaneous creation of localized excitations with a discontinuity in the partition function. The fact that this phenomenon is retained in the saturable DNLS is non-trivial, since in contrast to the cubic DNLS whose nonlinear character is enhanced as the excitation amplitude increases, the saturable DNLS in fact becomes increasingly linear as the excitation amplitude increases. We explore the nonlinear dynamics of this phenomenon by direct numerical simulations.

PACS numbers: 05.45.-a, 63.20.Pw, 63.70.+h

During the past two decades much research has been devoted to nonlinear mechanisms for the storage and transport of localized coherent packages of energy and charge in spatially periodic systems, which may be described by discrete lattice models in one, two, or three spatial dimensions [1–3]. Generally such systems may support intrinsic localized modes, or discrete breathers, which are time-periodic, spatially localized solutions to the dynamical lattice equations [4].

A much older interest [5] in such nonlinear systems arises from their ability to thermalize through their intrinsic dynamics leading to equipartition of excitation energy among the linear modes. Localization and equipartition appears somewhat contradictory and we have earlier explored their interrelation within the framework of the Discrete Nonlinear Schrödinger (DNLS) equation with a cubic nonlinearity [6, 7]. We found that in the case of the cubic DNLS these phenomena occur in distinct parameter domains. Thermalization in the Gibbsian sense occurs in the low energy part of the parameter space while the nonlinear dynamics for higher energies lead to the spontaneous creation of localized excitations prohibiting thermalization. It has been argued [8] that the statistical process behind this localization leads towards an entropy maximization. The entropy maximization is driven by optimally distributing the effects of fluctuations (which carry the main part of the system entropy) among different conserved quantities. Localization is therefore absent (Gibbsian regime) if insufficient energy is supplied by the initial conditions. If a surplus of energy is provided by the initial conditions, it is allotted to the high amplitude structures (non-Gibbsian regime) that absorb large amounts of energy while using few lattice positions. The specific separation of these two regimes was derived analytically [6].

Extending this prior work we will here detail a similar study for the DNLS with a saturable nonlinearity, which physically describes, e.g., discrete spatial solitons in a tight-binding approximation of one-dimensional optical waveguide arrays made from photorefractive crystals [9]. Another example where this equation arises is that of Bose-Einstein condensates in optical lattices [10]. Mathematically the saturable DNLS reduces to the cubic DNLS in the low amplitude (energy) limit, while it becomes essentially linear in the large amplitude limit. The saturable DNLS is known to support localized excitations [11–14], but it is unclear how the interplay of thermalization and spontaneous localization occurs in this case where strong localization essentially leads to linear dynamics.

To explore these issues we are concerned with the DNLS equation with a saturable nonlinearity

$$i\dot{\phi}_n + (\phi_{n+1} + \phi_{n-1}) + \frac{\nu|\phi_n|^2}{1+|\phi_n|^2}\phi_n = 0, \qquad (1)$$

or equivalently through the simple gauge transformation $\phi_n = \psi_n \exp(i\nu t)$

$$i\dot{\psi}_n + (\psi_{n+1} + \psi_{n-1}) - \frac{\nu\psi_n}{1+|\psi_n|^2} = 0, \qquad (2)$$

where ψ_n (ϕ_n) is a complex valued "wave function" at site n and ν is a real parameter that controls the nonlinearity of the system. It is important to note that for small excitation amplitudes $|\psi_n| \ll 1$ ($|\phi_n| \ll 1$) both equations reduce to the cubic DNLS.

Equation (2) represents a Hamiltonian system for the canonically conjugated pairs $i\psi_n$ and ψ_n^* with the Hamiltonian

$$\mathcal{H} = \sum_{n=1}^{N} \left[(\psi_n^*\psi_{n+1} + \psi_n\psi_{n+1}^*) - \nu \ln\left(1+|\psi_n|^2\right) \right], \qquad (3)$$

so that Eq. (2) is given by $i\dot{\psi}_n = -\frac{\partial \mathcal{H}}{\partial \psi_n^*}$. In addition to the Hamiltonian, $\mathcal{H}$, the quantity $\mathcal{A} = \sum_{n=1}^{N} |\psi_n|^2$ is also conserved by the dynamics of Eq. (2) and serves as the norm of the system.

Our objective is to calculate the grand-canonical partition function $\mathcal{Z}$ of this system and to accomplish this

we first apply the canonical transformation $|\psi_n|^2 = A_n$, $\psi_n = \sqrt{A_n}e^{i\theta_n}$, which brings the Hamiltonian $\mathcal{H}$ of Eq. (3) into the form

$$\mathcal{H} = \sum_{n=1}^{N} \left[2\sqrt{A_n A_{n+1}} \cos(\theta_n - \theta_{n+1}) - \nu \ln(1 + A_n) \right] \quad (4)$$

and the norm becomes $\mathcal{A} = \sum_{n=1}^{N} A_n$.

In terms of these variables the partition function $\mathcal{Z}$ is

$$Z = \prod_{n=1}^{N} \int_0^{2\pi} d\theta_n \int_0^{\infty} dA_n e^{-\beta(\mathcal{H}+\mu\mathcal{A})}, \quad (5)$$

where the parameter μ is introduced analogous to a chemical potential to ensure the conservation of $\mathcal{A}$. From this partition function all thermodynamic quantities of the system can be calculated. We will in particular be interested in the averaged norm density $a = \langle \mathcal{A} \rangle / N$ and the averaged energy density $h = \langle \mathcal{H} \rangle / N$, which are given by the following expressions

$$a = -\frac{1}{\beta N} \frac{\partial \ln Z}{\partial \mu}; \quad h + \mu a = -\frac{1}{N} \frac{\partial \ln Z}{\partial \beta}. \quad (6)$$

In Eq. (5) the integration over the phase variables θ_n can be preformed straightforwardly reducing the partition function to

$$\frac{Z}{(2\pi)^N} = \quad (7)$$
$$\prod_{n=1}^{N} \int_0^{\infty} dA_n I_0 \left(2\beta \sqrt{A_n A_{n+1}} \right) e^{-\beta\mu A_n} (1 + A_n)^{\beta\nu},$$

where I_0 denotes the modified Bessel function. Further treatment of the partition function has to be carried out numerically using for example the transfer integral approach [6]. However, in the two limits $\beta \to \infty$ and $\beta \to 0$ we can gain further analytical insight. Noticing that the Hamiltonian is bounded from below one can observe that its minimum (corresponding to $\beta \to \infty$) is realized by the plane wave $\psi_n = \sqrt{a} \exp in\pi$, whose energy density is $h = -2a - \nu \ln(1 + a)$. When $\beta \to 0$ while $\beta\mu$ remains finite the modified Bessel function in the expression for $\mathcal{Z}$ can reasonably be approximated by unity, which leads to

$$Z = (2\pi)^N \prod_{n=1}^{N} \int_0^{\infty} dA_n e^{-\beta\mu A_n} (1 + A_n)^{\beta\nu}. \quad (8)$$

Making the substitution $1 + A_n = x_n$ brings the partition function Z into

$$Z = (2\pi)^N e^{N\beta\mu} E(\beta\nu, \beta\mu)^N, \quad (9)$$

where the function $E(x, y)$ is given by

$$E(x, y) = \int_1^{\infty} du\, u^x\, e^{-yu}. \quad (10)$$

Keeping $\beta\mu = \gamma$ finite as we take the limits $\beta \to 0$ and $\mu \to \infty$, we can, using Eq. (6) and the properties for $E(x, y)$ listed in the appendix, obtain expressions for a and h

$$a = -\frac{1}{\beta} \left(\beta + \beta \frac{\partial \ln E(0, y)}{\partial y}\Big|_{y=\gamma} \right) \quad (11)$$
$$= -1 + \frac{E(1, \gamma)}{E(0, \gamma)} = -1 + 1 + \frac{1}{\gamma} = \frac{1}{\gamma}. \quad (12)$$

and

$$h + \mu a = -\mu - \nu \frac{\partial \ln E(x, \gamma)}{\partial x}\Big|_{x=0} - \mu \frac{\partial \ln E(0, y)}{\partial y}\Big|_{y=\gamma}$$
$$= -\mu - \frac{\nu}{E(0, \gamma)} \frac{\partial E(x, \gamma)}{\partial x}\Big|_{x=0} + \mu \left(1 + \frac{1}{\gamma} \right)$$
$$= \frac{\mu}{\gamma} - \nu \frac{\gamma}{e^{-\gamma}} \frac{E_1(\gamma)}{\gamma} = \mu a - \nu e^{\gamma} E_1(\gamma) \quad (13)$$

so that

$$h = -\nu\, e^{\gamma}\, E_1(\gamma) = -\nu\, e^{\frac{1}{a}}\, E_1\left(\frac{1}{a} \right). \quad (14)$$

We can now compare with the result of the cubic DNLS by considering small a. Using the last equality of Eq. (A.4) in the limit of small a, Eq. (14) becomes

$$h \simeq -\nu\, e^{\frac{1}{a}}\, a\, e^{\frac{-1}{a}}\, (1 - a) = -\nu a + \nu a^2. \quad (15)$$

In Fig. 1 we illustrate, for $\nu = 1$, these results in the (a, h)-plane. The thick lines represent $\beta = 0$ [Eq. (14)] and $\beta = \infty$ [$h = -2a - \nu \ln(1 + a)$] that bound the regime in which Gibbsian thermodynamics applies. The region below the minimum energy line $\beta = \infty$, is of course inaccessible and is therefore shaded. However, the region above the $\beta = 0$ line is accessible but cannot be captured by Gibbsian thermodynamics. In the corresponding region for the cubic DNLS we found [6] that the nonlinear dynamics lead to the spontaneous appearance of strongly localized discrete breather excitations. The dots overlaid on the $\beta = 0$ line represent values obtained numerically by applying the transfer integral technique (see details in Ref. [6]) to Eq. (8) using $\beta = 10^{-8}$. The numerical solution does not ignore the modified Bessel function in Eq. (8) and it therefore directly verifies the validity of the expression in Eq. (14). Finally, the dashed line illustrates the small amplitude approximation in Eq. (15), which corresponds to the cubic DNLS [15]. In order to explore the differences in the dynamics in the two regions separated by the $\beta = 0$ line we perform a number of direct numerical simulations of Eq.(2), with $\nu = 1$. These numerical simulations represent a micro-canonical ensemble since they are performed to conserve both norm and energy. We use initial conditions of the form $\psi_n = \sqrt{a} \exp(i\theta n)$, which can be realized in both regimes by tuning the wave number θ and the norm a. The energy of these initial conditions is given by $h = 2a \cos\theta - \ln(1 + a)$.

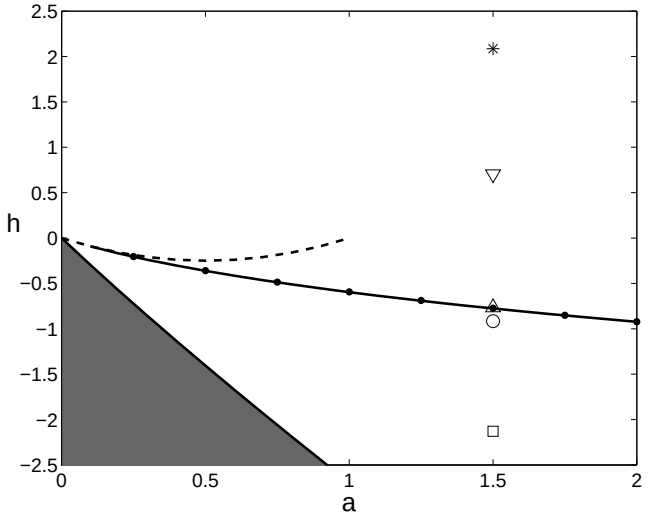

FIG. 1. Parameter space (a, h) [for $\nu = 1$], where the shaded area is inaccessible. The thick lines represent $\beta = 0$ [Eq.(14)] and $\beta = \infty$ [$h = -2a - \nu \ln(1 + a)$] and thereby bound the regime in which Gibbsian thermodynamics applies. The points are obtained numerically by applying the transfer integral technique to Eq. (8) using $\beta = 10^{-8}$. The dashed line represents Eq. (15) which corresponds to the cubic DNLS. Initial conditions for direct (micro-canonical) numerical calculations (see Figs. 2, 3, and 4) are marked by a square, a circle, an up-pointing triangle, a down-pointing triangle, and a star.

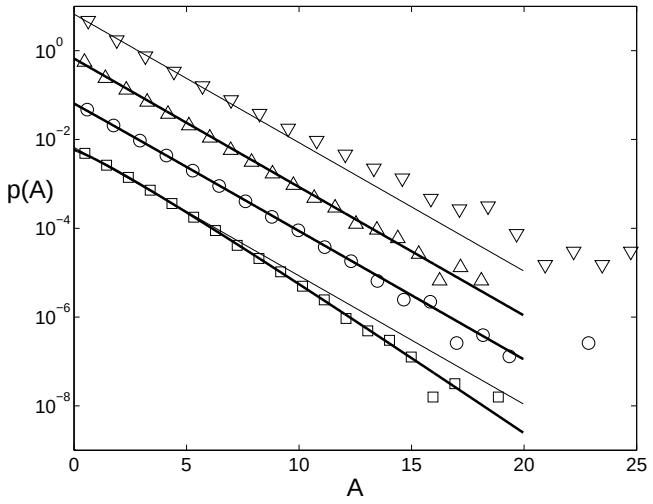

FIG. 2. Distributions of $A = |\psi_n|^2$ for four different energies at $a = 1.5$ [for $\nu = 1$]. The symbols show data obtained by direct numerical solution. Solid lines show the distribution function obtained by solution (using the transfer integral technique) of Eq. (8), while the thin lines show the function $\exp(-A/a)/a$. The curves have been shifted vertically to facilitate visualization. All data is for $a = 1.5$ while the energies are $h = -2.13$ (squares), $h = -0.97$ (circles), $h = -0.76$ (up-pointing triangles), and $h = 0.70$ (down-pointing triangles).

Our choices of initial conditions are marked in Fig. 1 and the result of simulations with these initial conditions are shown in Figs. 2 and 3. Figure 2 shows the amplitude distributions $p(A)$ resulting from long-time simulations. The numerically obtained distributions are shown with triangles, circles, and squares while the distribution functions obtained by the transfer integral approach are shown with thick lines. The thin lines show the function $\exp(-A/a)/a$. As the above analytical work demonstrates, this function approximates the distribution function in the limit of small β. The validity of this approximation is clearly verified by Fig. 2 since the thin lines are only discernible for β sufficiently large. Figure 2 also clearly demonstrates that the distribution arising from initial conditions above the $\beta = 0$ line are significantly different from the Gibbsian distribution functions. While the Gibbsian distribution functions are concave the non-Gibbsian distribution functions are convex and have significant tails at large values of A. This convexity is reminiscent of the discussion in Ref. [6] regarding "negative temperatures" and is a subject that recently has been discussed in more detail [16] in this context. These features are even more pronounced in the example given in Fig. 3 which originates from initial conditions located deep within the non-Gibbsian regime. The long tail distributions indicate the presence of a large amplitude excitations in the dynamics. The abrupt drop in

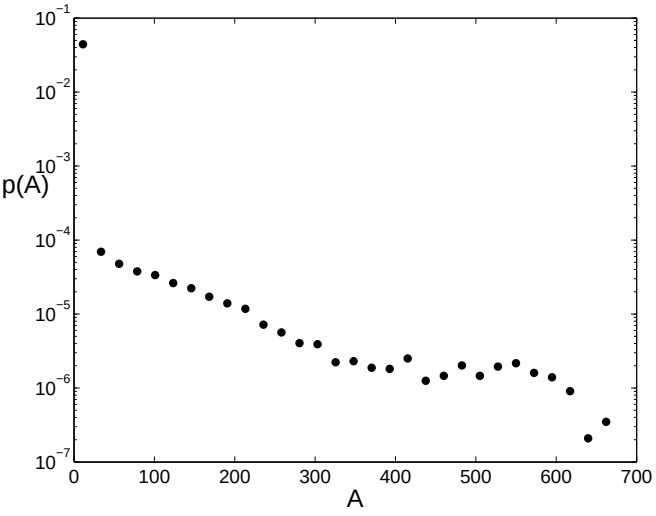

FIG. 3. Distributions of $A = |\psi_n|^2$ for $h = 2.09$ at $a = 1.5$ [for $\nu = 1$]. The distribution is obtained by direct numerical solution of Eq. (2).

the distribution function at very small excitation amplitudes clearly shows that the large amplitude excitations exist on an extensive background of small amplitude excitations. This scenario is quite similar to Rumpf's [8] description of the dynamics of the cubic DNLS in this regime, which in turn suggests that also in this case does localized high-amplitude excitations absorb a surplus of

energy when they emerge as a consequence of the production of entropy in the small uctuations.

In Fig. 4 we directly illustrate these excitations with a spatio-temporal snapshot of the dynamics. A few very large amplitude excitations occur early in the dynamics. These excitations are much larger in amplitude than what is typically observed in the cubic DNLS and although they are very discrete, only spanning 1-3 sites they are highly mobile [14]. This mobility allows the excitations to collide and these collisions appear to lead to further amplitude enhancement. In spite of this high mobility the probability distribution function still reaches stationarity very slowly and require integration times above 10^6 time units.The process remains slow because the collisions become quite rare as the excitation amplitudes increase.

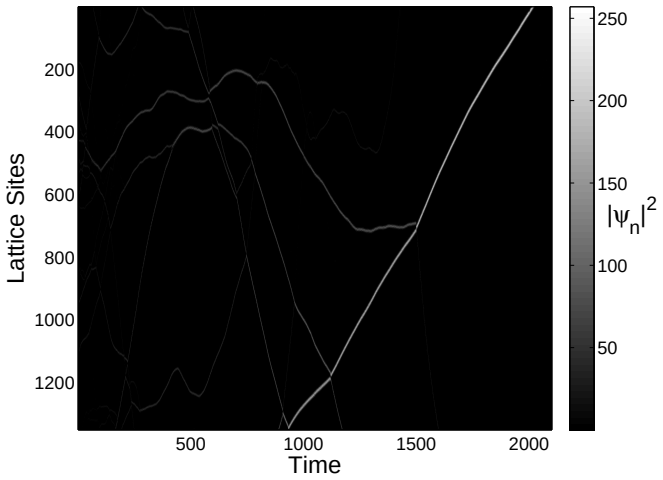

FIG. 4. (Color online) Spatio-temporal snapshot of the dynamics in the strongly non-Gibbssian regime for $h = 2.09$ at $a = 1.5$ [for $\nu = 1$].

In summary, we have studied a nonlinear Schrödinger equation with saturable nonlinearity, and derived the separation between Gibbsian and non-Gibbsian regime in the (a, h) phase space. Through analytical calculations supported by direct numerical simulations we have, as in the case of the cubic DNLS, been able to link the non-Gibbsian regime to the appearance of localized modes. The fact that this phenomenon is retained in the saturable DNLS is significant since in contrast to the cubic DNLS whose nonlinear character is enhanced as the excitation amplitude increases the saturable DNLS in fact becomes increasingly linear as the excitation amplitude increases.

ACKNOWLEDGMENTS

This research was carried out under the auspices of the National Nuclear Security Administration of the US Department of Energy at Los Alamos National Laboratory under Contract No. DE-AC52-06NA25396.

Appendix: Properties of $E(x, y)$

Some specific properties of the function $E(x, y)$ and its derivatives:

$$E(x,y) = \int_1^\infty u^x e^{-yu} du \qquad (A.1)$$
$$= e^{-y} \int_0^\infty e^{-yz + x\ln(1+z)}\, dz.$$

For the n'th derivative of $E(x, y)$ with respect to x we find

$$\frac{\partial^n E(x,y)}{\partial x^n} = e^{-y} \int_0^\infty (\ln(1+z))^n e^{-yu + x\ln(1+z)}\, dz, \qquad (A.2)$$

and for the n'th derivative of $E(x, y)$ with respect to y we find

$$\frac{\partial^n E(x,y)}{\partial y^n} = (-1)^n \int_1^\infty u^{x+n} e^{-yu + x\ln u}\, du \qquad (A.3)$$
$$= (-1)^n E(x+n, y).$$

Using these expressions we find the following

$$E(0,y) = \frac{e^{-y}}{y}; \quad E(1,y) = \frac{e^{-y}}{y}\left(1 + \frac{1}{y}\right) \qquad (A.4)$$

and

$$\frac{\partial E(x,y)}{\partial x}\Big|_{x=0} = e^{-y} \int_0^\infty \ln(1+z) e^{-yu}\, dz, \qquad (A.5)$$
$$= e^{-y} \int_0^\infty \left(z - \frac{z^2}{2} + \frac{z^3}{3} - \cdots\right) e^{-yz}\, dz.$$
$$= \frac{e^{-y}}{y^2}\left(1 - \frac{1}{y} + \frac{2}{y^2} - \cdots\right) = \frac{E_1(y)}{y}.$$

The last expression follows for example from Eq. (5.1.51) of Ref. [17] where the exponential integral is defined as $E_1(y) = \int_y^\infty \frac{e^{-t}}{t} dt$ (see Eq. 5.1.1 of Ref. [17]).

[1] P.G. Kevrekidis, K.Ø. Rasmussen, and A.R. Bishop, Int. J. Mod. Phys. B **15**, 2833, (2001).

[2] P.G. Kevrekidis, (Ed.), The Discrete Nonlinear Schrö dinger Equation. Mathematical Analysis, Numerical Computations and Physical Perspectives, (Springer, Berlin, 2009).

[3] S. Flach and A.V. Gorbach, Phys. Rep. **467**, 1, (2008).

[4] R.S. MacKay and S. Aubry, Nonlinearity **7**, 1623 (1994).

[5] E. Fermi, J. Pasta, and S. Ulam, Lect. Appl. Math **15**, 143 (1974).

[6] K.Ø. Rasmussen, T. Cretegny, P.G. Kevrekidis, and Niels Grønbech-Jensen, Phys. Rev. Lett. **84**, 3740 (2000).

[7] M. Johansson and K. Ø. Rasmussen, Phys. Rev. E **70**, 066610 (2004).
[8] B. Rumpf, Phys. Rev. E **69**, 016618 (2004).
[9] F. Lederer, G. I. Stegeman, D. N. Christodoulides, G. Assanto, M. Segev, and Y. Silberberg, Phys. Rep. **463**, 1, (2008).
[10] A. Trombettoni and A. Smerzi, Phys. Rev. Lett. **86**, 2353 (2001).
[11] A. Khare, K.Ø. Rasmussen, M. R. Samuelsen, and A. Saxena, J. Phys. **A38**, 807 (2005).
[12] A. Khare , K.Ø. Rasmussen, M. R. Samuelsen, and A. Saxena J. Phys. **A42**, 085002, (2009).
[13] T.R.O. Melvin, A.R. Champneys, P.G. Kevrekidis, and J. Cuevas, Phys. Rev. Lett. **97**, 124101 (2006).
[14] M. Syafwan, H. Susanto, S. M. Cox, and B. A. Malomed, J. Phys. A: Math. Theor. **45**, 075207 (2012).
[15] When comparing these results to the results for the cubic DNLS presented in Ref. [6] it is important to note that Eq. (2) contains the additional $-\nu\psi$ term in the small amplitude limit compared to the corresponding equation in Ref. [6]. This term accounts for the $-\nu a$ term in Eq. (15).
[16] S. Lubini, R. Franzosi, R. Livi, G.-L. Oppo, and A. Politi, New Journal of Physics **15**, 023032 (2013).
[17] *Handbook of Mathematical Functions with Formulas, Graphs, and Mathematical Tables*, edited by M. Abramowitz and I. A. Stegun (U.S. GPO, Washington, D.C., 1964).